

Mechanism of hyperscaling violation in the 2D 8-state Potts model with long-range correlated disorder

Christophe Chatelain

*School of Physics, Indian Institute of Science Education and Research (IISER), Thiruvananthapuram, India and
Groupe de Physique Statistique, Département P2M,
Institut Jean Lamour (CNRS UMR 7198), Université de Lorraine, France*

(Dated: March 15, 2013)

The first-order phase transition of the two-dimensional eight-state Potts model is shown to be rounded when long-range correlated disorder is coupled to energy density. Critical exponents are estimated by means of large-scale Monte Carlo simulations. In contrast to uncorrelated disorder, a violation of the hyperscaling relation $\gamma/\nu = d - 2x_\sigma$ is observed. This violation is caused by large disorder fluctuations, like in the 3D random field Ising model. In the thermal sector too, evidences are given for such violation in the two hyperscaling relations $\alpha/\nu = d - 2x_\epsilon$ and $1/\nu = d - x_\epsilon$. The scaling dimension of energy is conjectured to be $x_\epsilon = a/2$, where a is the exponent of the algebraic decay of disorder correlations.

PACS numbers: PACS numbers: 64.60.De, 05.50.+q, 05.70.Jk, 05.10.Ln

Quenched disorder when coupled to the energy density, say by dilution or random couplings, is known to soften first-order phase transitions. As argued by Imry and Wortis [1], local fluctuations of impurity concentration can destabilize the ordered phases in coexistence at the transition temperature if the surface tension is sufficiently small. In 2D, it was rigorously proved that an infinitesimal amount of disorder is sufficient to make any first-order transition continuous [2, 3]. The complete vanishing of the latent heat was first observed numerically in the case of the 2D 8-state Potts model [4]. The critical behavior of the disorder-induced second-order phase transition is governed by a new random fixed point [5]. The universality class was later shown to depend on the number of states q [6]. In 3D, a finite disorder is required to round completely the first-order phase transition. The phase diagram exhibits a tricritical point separating a first-order regime from the disorder-induced continuous one, as first observed in the bond-diluted 4-state Potts model [7]. A rounding of the first-order phase transition of the 2D Potts model was also reported for anisotropic aperiodic sequences of couplings [8], and for layered random couplings [9, 10]. In both cases, the couplings are infinitely correlated in one direction. In the random case, the critical behavior was shown to be governed by a q -independent infinite-randomness fixed point. The critical exponents are therefore those of the layered random Ising model, the celebrated McCoy-Wu model [11, 12]. Interestingly, the same critical behavior is observed for the Potts model with homogeneous uncorrelated disorder in the limit $q \rightarrow +\infty$ [13]. Hyperscaling holds for all these models.

In the following, we consider random bond couplings $J_{ij} > 0$ with algebraically decaying correlations $\overline{(J(0) - \bar{J})(J(\vec{r}) - \bar{J})} \sim r^{-a}$. A simple generalization of the Imry-Wortis criterion shows that the low-temperature phase is destabilized when the coupling fluc-

tuations, inside a domain of characteristic length ℓ ,

$$\sqrt{(J - \bar{J})^2} \sim \left[\ell^d \int_{\ell^d} \frac{d^d \vec{r}}{r^a} \right]^{1/2} \sim \ell^{d-a/2}, \quad (a < d) \quad (1)$$

increase faster with ℓ than the interface free energy $\sigma \ell^{d-1}$. In the two-dimensional case, we expect the first-order phase transition to be softened for $a \leq 2$.

We consider the 2D q -state Potts model with Hamiltonian

$$-\beta H = \sum_{(i,j)} J_{ij} \delta_{\sigma_i, \sigma_j} \quad (2)$$

where $\sigma_i \in \{0, 1, \dots, q-1\}$ and the sum extends over pairs of nearest neighbors of the square lattice. We restrict ourselves to the case $q = 8$ for which the correlation length of the pure model is $\xi \simeq 24$ at the transition temperature. We considered a binary distribution of coupling constants $J_{ij} \in \{J_1, J_2\}$ with

$$(e^{J_1} - 1)(e^{J_2} - 1) = q. \quad (3)$$

In the case of uncorrelated disorder, Eq. (3) is the self-duality condition that gives the location of the critical line. The ratio $r = J_2/J_1$ is used as a measure of the strength of disorder. Here, we presents results for the case $r = 8$. To generate correlated coupling configurations $\{J_{ij}\}$, we simulate another spin model, namely the Ashkin-Teller model ($\sigma_i, \tau_i = \pm 1$)

$$-\beta H^{\text{AT}} = \sum_{(i,j)} [J^{\text{AT}} \sigma_i \sigma_j + J^{\text{AT}} \tau_i \tau_j + K^{\text{AT}} \sigma_i \sigma_j \tau_i \tau_j] \quad (4)$$

at different points of its critical line $e^{-2K^{\text{AT}}} = \sinh 2J^{\text{AT}}$. Two symmetries of the Hamiltonian are spontaneously broken at low temperatures: the global reversal of the spins σ_i and the reversal of both σ_i and τ_i . Therefore, two order parameters can be defined, magnetization $\sum_i \sigma_i$ and polarization $\sum_i \sigma_i \tau_i$, leading to two independent scaling dimensions $\beta_\sigma^{\text{AT}} = \frac{2-y}{24-16y}$ and $\beta_{\sigma\tau}^{\text{AT}} =$

$\frac{1}{12-8y}$ wherein we use the parametrization $\cos \frac{\pi y}{2} = \frac{1}{2} \left[e^{4K^{\text{AT}}} - 1 \right]$ ($y \in [0; 4/3]$). The correlation length exponent is $\nu^{\text{AT}} = \frac{2-y}{3-2y}$. Spin configurations of this model are generated by Monte Carlo simulation using a cluster algorithm [14]. For each of them, a coupling configuration of the Potts model is constructed as

$$J_{ij} = \frac{J_1 + J_2}{2} + \frac{J_1 - J_2}{2} \sigma_i \tau_i, \quad (5)$$

where the site j is either at the right or below the site i . By construction, disorder fluctuations are self-similar and the coupling constants display algebraic correlations $(J_{ij} - \bar{J})(J_{kl} - \bar{J}) \sim |\vec{r}_i - \vec{r}_k|^{-a}$ at large distances with $a = 2\beta_{\sigma\tau}^{\text{AT}}/\nu^{\text{AT}} = 1/(4-2y)$. We have considered six points on the critical line, $y \in \{0, 0.25, 0.50, 0.75, 1, 1.25\}$, leading to six correlated disorder distributions with $a \simeq 0.25, 0.286, 0.333, 0.4, 0.5$ and 0.667 . Note that for $y = 0$, the Ashkin-Teller model is equivalent to the 4-state Potts model. The critical behavior is therefore affected by logarithmic corrections. Finally note that this construction ensures that the constraint (3) implies the self-duality of our random Potts model.

The Potts model is then simulated using the Swendsen-Wang algorithm [15]. Lattice sizes between $L = 16$ and 256 are considered. For each disorder configuration, 1000 MCS are performed to thermalize the system and 20,000 MCS for data accumulation (auto-correlation time is $\tau \simeq 2$ for $L = 256$). Thermodynamic quantities are averaged over a number of disorder configurations proportional to $1/L^2$. For the largest lattice size $L = 256$, 2560 disorder configurations are generated while for $L = 64$ for instance, this number is raised up to 40960. Stability of disorder averages is checked. In the following, we will denote $\langle X \rangle$ the average of an observable over thermal fluctuations and $\overline{\langle X \rangle}$ the average of the latter over disorder.

On the critical line, the typical spin configurations of the Ashkin-Teller model display a large cluster of polarization $\sigma\tau = +1$ or -1 . As a consequence, our random coupling configurations also exhibit large clusters of either strong or weak bonds. The probability distribution of the total energy of the Potts model shows two peaks corresponding to these two kinds of bond configurations. This distribution is highly correlated to the probability distribution of polarization of the Ashkin-Teller model. Since the latter undergoes a second-order phase transition, the two peaks come closer as the lattice size is increased. Note that in our model, macroscopic region of strong couplings are not rare: they have a probability $1/2$. Moreover, they have a fractal dimension $1 < d_f < 2$ determined by the Ashkin-Teller model and, in the thermodynamic limit, only one such macroscopic region is expected to be present in the system. For this reason, the transition is not smeared but rounded [16].

We estimate critical exponents by Finite-Size Scaling.

The exponent β/ν can be extracted from magnetization $\overline{\langle m \rangle}$ and its moments $\overline{\langle m^n \rangle}$ with $n = 2, 3, 4$. We observe nice power laws without any significant correction to scaling. Our estimates of $x_\sigma = \beta/\nu$ evolve with a and range from $0.061(5)$ ($y = 0$) to $0.108(4)$ ($y = 1.25$), to be compared with $0.150(2)$ for uncorrelated disorder (Tab. I). We then consider the average magnetic susceptibility, numerically computed via the fluctuation-dissipation theorem $\bar{\chi} = L^d \overline{\langle m^2 \rangle} - \overline{\langle m \rangle}^2$. The data display large corrections to scaling (see Fig. 1). A cross-over is observed around $L = 48$, not far from the correlation length $\xi = 24$ of the pure 8-state Potts model. In the region $L \geq 96$, power-law interpolations give stable estimates for γ/ν going from $1.70(7)$ ($y = 0.00$) to $1.62(4)$ ($y = 1.25$), to be compared with $1.69(4)$ for uncorrelated disorder. The hyperscaling relation $\gamma/\nu = d - 2\beta/\nu$ is therefore not satisfied. We shall identify disorder fluctuations as the origin of this hyperscaling violation, like in the 3D Random-Field Ising Model (RFIM). Consider the following decomposition:

$$\bar{\chi} = L^d [\overline{\langle m^2 \rangle} - \overline{\langle m \rangle}^2] - L^d [\overline{\langle m \rangle^2} - \overline{\langle m \rangle}^2]. \quad (6)$$

The first term, when computed separately, displays a power law behavior with an exponent $(\gamma/\nu)^*$ incompatible with γ/ν but in agreement with the hyperscaling relation (Tab. I). The second term of (6), the so-called disconnected susceptibility, involves the ratio

$$R_m = \frac{\overline{\langle m \rangle^2} - \overline{\langle m \rangle}^2}{\overline{\langle m \rangle^2}}, \quad (7)$$

which is expected to behave as $R_m \sim R_m(\infty) + \mathcal{A}L^{-\phi}$, if magnetization is not self-averaging [17]. We indeed observe that R_m goes to a non-vanishing constant in the limit $L \rightarrow +\infty$ (Fig. 2). The second term of Eq. (6) therefore behaves as $L^d \overline{\langle m \rangle^2} \sim L^{d-2\beta/\nu}$, i.e. with an exponent satisfying the hyperscaling relation. Since the data indicate that it is also the case for the first term of Eq. (6), one can imagine that, if their amplitudes are equal, the dominant terms will cancel. To test this hypothesis, we compute the ratio

$$\frac{\overline{\langle m^2 \rangle} - \overline{\langle m \rangle}^2}{\overline{\langle m \rangle^2} - \overline{\langle m \rangle}^2}. \quad (8)$$

We observe a plateau at $1.00(4)$ (Fig. 2). We therefore conclude that the hyperscaling violation is the result of an exact cancellation of the dominant contributions of the two terms of Eq. (6). The scaling of the average susceptibility is therefore determined by the first non-vanishing scaling correction $\bar{\chi} \sim L^{d-2\beta/\nu-\omega}$ of any of the two terms of Eq. (6) and the hyperscaling violation exponent θ is the exponent ω of this correction. Note that this is also the mechanism of hyperscaling violation invoked in the context of the RFIM [18] where our exponent $(\gamma/\nu)^*$ is

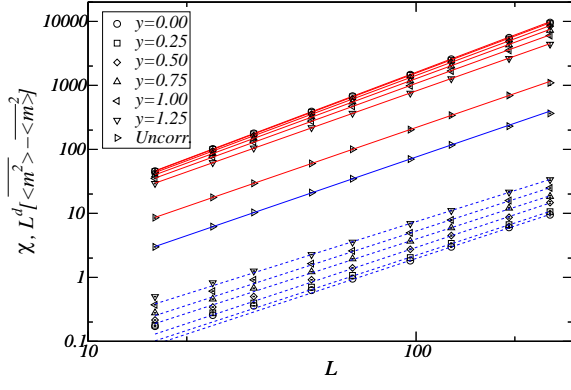


FIG. 1. Average magnetic susceptibility $\bar{\chi}$ (bottom) and $L^d[\langle m^2 \rangle - \langle m \rangle^2]$ (top) versus lattice size L for different values of y and uncorrelated disorder (Uncorr.). The dashed line indicates that the fit is performed over lattice sizes $L \geq 96$ only.

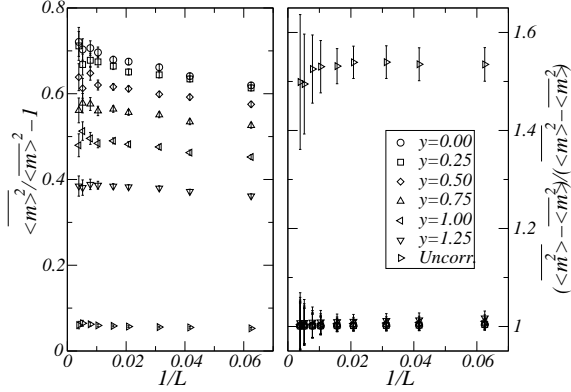


FIG. 2. Ratios defined by Eq. (7) on the left and (8) on the right versus the inverse of the lattice size.

denoted $4 - \bar{\eta}$ [19]. In the case of uncorrelated disorder, the ratio (8) goes to a value significantly different from 1 in the large size limit (Fig. 2). The dominant contribution of the two terms of (6) do not cancel in this case and therefore hyperscaling is not violated.

The divergence of specific heat is completely washed out by the introduction of disorder, which means that the specific heat exponent α/ν is zero or negative (Fig 3). $\bar{C} = L^d \langle e^2 \rangle - \langle e \rangle^2$ can be decomposed in the same way as $\bar{\chi}$:

$$\bar{C} = L^d [\langle e^2 \rangle - \langle e \rangle^2] - L^d [\langle e^2 \rangle - \langle e \rangle^2]. \quad (9)$$

We observe a nice power-law behavior of the first term with an exponent in good agreement with $(\alpha/\nu)^* = (\gamma/\nu)^{\text{AT}} = d - a$, which means that the fluctuations of energy are dominated by the fluctuations of the couplings and therefore of the polarization density in the original Ashkin-Teller model. The second term involves the ratio R_e , constructed in the same way as R_m (7). Our numerical data show that energy is not self-averaging

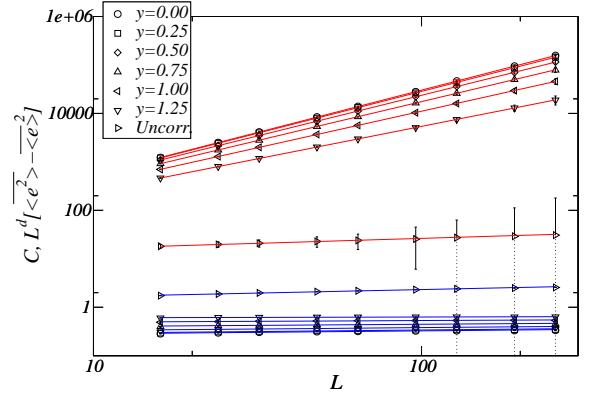


FIG. 3. Average specific heat \bar{C} (bottom) and $L^d[\langle e^2 \rangle - \langle e \rangle^2]$ (top) versus lattice size L for different values of y and uncorrelated disorder (Uncorr.). For clarity, error bars of \bar{C} in the uncorrelated case have been drawn as dashed line when they overlap with other points.

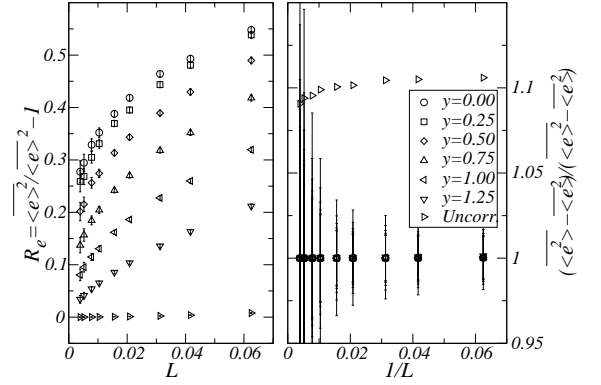


FIG. 4. Ratios defined in the same way as Eq. (7) on the left and (8) on the right but for energy instead of magnetization. On the right, the error bars for uncorrelated disorder are large (they overlap other bars for large lattice sizes) and have not been represented for clarity.

($R_e(\infty) \neq 0$) and the ratio $\frac{\langle e^2 \rangle - \langle e \rangle^2}{\langle e \rangle^2 - \langle e \rangle^2}$ exhibits a plateau at the value 1.00(5) (Fig. 4). This implies the cancellation of the dominant contribution of the two terms of \bar{C} so that a violation of the hyperscaling relation $\alpha/\nu = d - 2x_e$ is expected. Even though we cannot measure x_e from the scaling behavior of energy, we infer that it can be extracted from the hyperscaling relation $(\alpha/\nu)^* = d - 2x_e$ which implies $x_e = a/2$. In the case of uncorrelated disorder, R_e is compatible with zero which means that energy is self-averaging and therefore the two dominant contributions of Eq. (9) do not cancel. As observed, hyperscaling is not violated in this case.

In pure systems, a good estimator for the determination of the correlation exponent ν is $-\frac{d \ln \langle m \rangle}{d\beta} = L^d \frac{\langle m e \rangle - \langle m \rangle \langle e \rangle}{\langle m \rangle}$. This is generalized to random systems

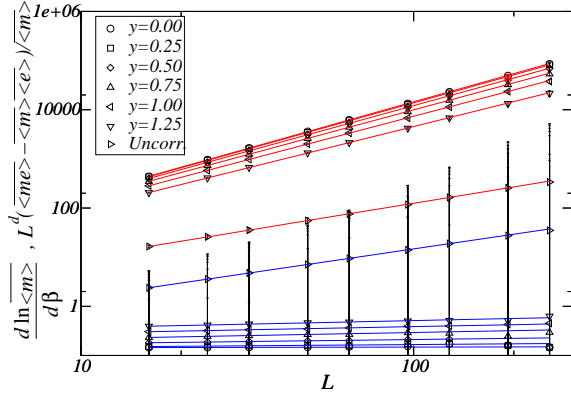


FIG. 5. Quantity $-\frac{d \ln \overline{m}}{d\beta}$ (bottom) and $L^d \frac{\overline{me} - \overline{m} \langle e \rangle}{\overline{m}}$ (top) versus lattice size L for different values of y and uncorrelated disorder (Uncorr.).

as:

$$-\frac{d \ln \overline{m}}{d\beta} = L^d \frac{\overline{me} - \overline{m} \langle e \rangle}{\overline{m}}. \quad (10)$$

and is expected to scale as $d - x_\epsilon$. A power-law interpolation of our data gives exponents $1/\nu$ close to zero but with large error bars. Consider again the decomposition

$$-\frac{d \ln \overline{m}}{d\beta} = L^d \frac{\overline{me} - \overline{m} \langle e \rangle}{\overline{m}} - L^d \frac{\overline{m} \langle e \rangle - \overline{m} \langle e \rangle}{\overline{m}}. \quad (11)$$

The first term displays a power-law behavior with exponents $1/\nu^*$ close to, though slightly above, $d - x_\epsilon$, which implies $x_\epsilon \simeq a/2$ (Tab. I). This estimate is consistent with the one obtained from the specific heat. The second term of (11) involves the ratio

$$R_{me} = \frac{\overline{me} - \overline{m} \langle e \rangle}{\overline{m} \langle e \rangle}, \quad (12)$$

which behaves as $R_{me}(L) \sim R_{me}(\infty) + aL^{-\phi'}$ with $\phi' \simeq 0.3$. The constant $R_{me}(\infty)$ is clearly finite, except maybe for $y = 1.25$. Like in the magnetic case, the two terms of Eq. (11) have the same dominant scaling behavior. The ratio

$$\frac{\overline{me} - \overline{m} \langle e \rangle}{\overline{m} \langle e \rangle - \overline{m} \langle e \rangle} \quad (13)$$

displays a plateau at 1.00(4) (Fig. 6). Consequently, the dominant contribution of the two terms of (11) is the same and they cancel. Hence, the hyperscaling relation $1/\nu = d - x_\epsilon$ is expected to be violated. In the case of uncorrelated disorder, R_{me} is compatible with zero so we do not expect any cancellation of the two dominant contributions of Eq. (11) and, consequently, no hyperscaling violation.

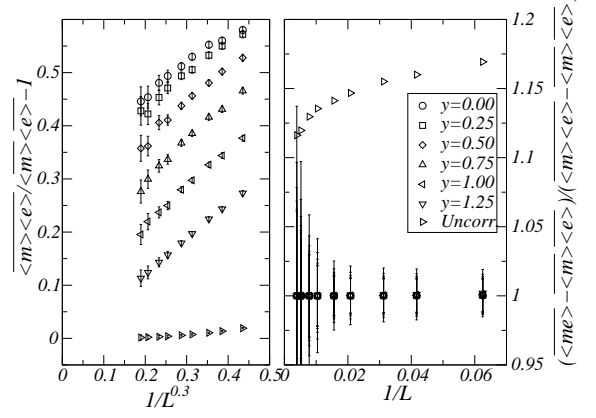


FIG. 6. Ratios defined by Eq. (12) on the left and (13) on the right. On the right, the error bars for uncorrelated disorder are large and have not been represented for clarity.

y	0	0.25	0.5	0.75	1	1.25
a	0.25	0.286	0.333	0.4	0.5	0.667
β/ν	0.061(5)	0.060(5)	0.067(5)	0.075(5)	0.091(5)	0.108(4)
$d - 2\beta/\nu$	1.88(1)	1.88(1)	1.87(1)	1.85(1)	1.82(1)	1.784(8)
γ/ν	1.70(7)	1.69(8)	1.69(7)	1.67(8)	1.66(6)	1.62(5)
$(\gamma/\nu)^*$	1.91(2)	1.90(3)	1.89(3)	1.87(3)	1.83(3)	1.79(3)
$(\alpha/\nu)^*$	1.75(1)	1.73(2)	1.68(2)	1.61(2)	1.51(2)	1.34(2)
$d - a$	1.75	1.714	1.667	1.600	1.500	1.333
$1/\nu^*$	1.90(2)	1.89(2)	1.86(2)	1.83(2)	1.78(2)	1.69(2)
$d - a/2$	1.875	1.857	1.835	1.8	1.75	1.667

TABLE I. Critical exponents measured by Monte Carlo simulations, or computed from them, and conjectured values.

Finally, note that, in contrast to the RFIM, at least two hyperscaling violation exponents are needed to explain the numerical data presented in this letter. In the magnetic sector, the hyperscaling violation exponent is estimated to be $\theta = (\gamma/\nu)^* - (\gamma/\nu) \simeq 0.2$ while in the energy sector, $\theta = (\alpha/\nu)^* - (\alpha/\nu) \gtrsim d - a$.

The author gratefully thanks Sreedhar Dutta and the Indian Institute for Science Education and Research (IISER) of Thiruvananthapuram for their warm hospitality and a stimulating environment.

-
- [1] Y. Imry and M. Wortis *Phys. Rev. B* **19** 3580 (1979).
 - [2] K. Hui and A.N. Berker *Phys. Rev. Lett.* **62** 2507 (1989); K. Hui and A.N. Berker *Phys. Rev. Lett.* **63** 2433 (1989).
 - [3] M. Aizenman and J. Wehr *Phys. Rev. Lett.* **62** 2503 (1989); M. Aizenman and J. Wehr *Comm. Math. Phys.* **130** 489 (1990).
 - [4] S. Chen, A.M. Ferrenberg and D. P. Landau *Phys. Rev. Lett.* **69** 1213 (1992); S. Chen, A.M. Ferrenberg, and D. P. Landau *Phys. Rev. E* **52** 1377 (1995).
 - [5] C. Chatelain, and B. Berche *Phys. Rev. Lett.* **80** 1670 (1998).

- [6] T. Olson, and A.P. Young *Phys. Rev. B* **60** 3428 (1999),
C. Chatelain, and B. Berche *Phys. Rev. E* **60** 3853 (1999),
J.L. Jacobsen, and M. Picco *Phys. Rev. E* **61** R13 (2000).
- [7] C. Chatelain, B. Berche, W. Janke, and P.-E. Berche
Phys. Rev. E **64** 036120 (2001).
- [8] P.-E. Berche, C. Chatelain and B. Berche *Phys. Rev.
Lett.* **80** 297 (1998).
- [9] T. Senthil and S.N. Majumdar *Phys. Rev. Lett.* **76** 3001
(1996).
- [10] E. Carlon, C. Chatelain and B. Berche *Phys. Rev. B* **60**
12974 (1999).
- [11] B.M. McCoy and T.T. Wu *Phys. Rev.* **176** 631 (1968);
B.M. McCoy and T.T. Wu *Phys. Rev.* **188** 982 (1969).
- [12] D.S. Fisher *Phys. Rev. B* **51** 6411 (1995).
- [13] J-Ch. Anglès d'Auriac and F. Iglói *Phys. Rev. Lett.* **90**
190601 (2003); M.T. Mercaldo, J-Ch. Anglès d'Auriac
and F. Iglói *Phys. Rev. E* **69** 056112 (2004).
- [14] J. Salas and A.D. Sokal *J. Stat. Phys.* **85** 297 (1996).
- [15] R.H. Swendsen, and J.S. Wang *Phys. Rev. Lett.* **58** 86
(1987).
- [16] T. Vojta *J. Phys. A.* **39** R143 (2006).
- [17] S. Wiseman, and E. Domany *Phys. Rev. E* **52** 3469
(1995).
- [18] M. Schwartz, and A. Soffer *Phys. Rev. Lett.* **55** 2499
(1985).
- [19] A.J. Bray, and M.A. Moore *J. Phys. C* **18** L927 (1985).